

A W-band high-gain and low-noise amplifier MMIC using InP-based HEMTs

ZHONG Ying-Hui¹, LI Kai-Kai¹, LI Xin-Jian¹, JIN Zhi^{2*}

(1. School of Physics and Engineering, Zhengzhou University, Zhengzhou 450001, China;

2. Institute of Microelectronics, Chinese Academy of Sciences, Beijing 100029, China)

Abstract: In this paper, a single-stage W-band low noise amplifier (LNA) monolithic millimeter-wave integrated circuit (MMIC) has been designed and fabricated using our own InP-based high electron mobility transistor technology. The LNA MMIC is developed in Cascode topology and coplanar waveguide technology, which result in a very compact chip with size of $900\ \mu\text{m} \times 975\ \mu\text{m}$ and a rather high linear gain over 10 dB from 84 GHz to 100 GHz with the maximum value of 15.2 dB at 95 GHz. To our knowledge, this single-stage LNA MMIC exhibits the highest gain-per-stage and competitive gain-area ratio among reported W-band LNA MMICs. Additionally, the amplifier also demonstrates a relatively low noise figure of 4.3 dB at 87.5 GHz and a fairly high saturated output power of 8.03 dBm at 88.8 GHz at room temperature. The successful fabrication of LNA MMIC is of great significance on building a W-band signal receiver-front-end system.

Key words: high electron mobility transistor (HEMT), low noise amplifier, InP, cascode

PACS: 84.40.Dc, 85.30.Tv

基于 InP 基 HEMTs 的 W 波段高增益低噪声放大 MMIC

钟英辉¹, 李凯凯¹, 李新建¹, 金智^{2*}

(1. 郑州大学 物理工程学院, 郑州 450001; 2. 中国科学院微电子研究所, 北京 100029)

摘要: 基于自主研发的 InP 基高电子迁移率晶体管工艺设计并制作了一款 W 波段单级低噪声放大单片毫米波集成电路。共源共栅拓扑结构和共面波导工艺保证了该低噪声放大器紧凑的面积和高的增益, 其芯片面积为 $900\ \mu\text{m} \times 975\ \mu\text{m}$, 84 ~ 100 GHz 频率范围内增益大于 10 dB, 95 GHz 处小信号增益达到最大值为 15.2 dB。根据调查对比, 该单级放大电路芯片具有最高的单级增益和相对高的增益面积比。另外, 该放大电路芯片在 87.5 GHz 处噪声系数为 4.3 dB, 88.8 GHz 处饱和输出功率为 8.03 dBm。该低噪声放大器芯片的成功研制对于构建一个 W 波段信号接收前端具有重要的借鉴意义。

关键词: 高电子迁移率晶体管; 低噪声放大电路; 磷化铟; 共源共栅

中图分类号: TN432 **文献标识码:** A

Introduction

Recently, millimeter-wave systems have rapidly emerged as potential candidate for various attractive demands, such as 60 GHz short-range communication^[1], 77 GHz automotive radar systems^[2] and 94 GHz high-resolution imaging applications^[3]. The ultimate sensitivity and noise characteristic of these instruments depend more strongly on low noise amplifier (LNA) monolithic millimeter-wave integrated circuits (MMICs) than any

other building blocks. As a result, LNA MMICs possessing high gain, low noise figure, wide bandwidth, become as a critical component in nearly all millimeter-wave applications. Because of high carrier peak drift velocity, high carrier low-field mobility and high carrier sheet density in InGaAs channel, InP-based high electron mobility transistor (HEMT) demonstrates extremely excellent characteristics, such as high frequency, low noise figure, and superior gain performance and so on. Consequently, many excellent W-band LNA MMICs have been developed in InP-based HEMT technology^[4-5], which

Received date: 2014 - 09 - 28, **revised date:** 2015 - 10 - 04

收稿日期: 2014 - 09 - 28, **修回日期:** 2015 - 10 - 04

Foundation items: Supported by National Natural Science Foundation of China (61404115, 61434006)

Biography: ZHONG Ying-Hui (1987-), female, China, Ph. D. Research fields are fabrication of millimeter-wave devices, circuits, modeling, and irradiation effects. E-mail: zhongyinghui401@163.com

* **Corresponding author:** E-mail: jinzhi@ime.ac.cn

benefit from extraordinarily exquisite manufacturing technology and astonishingly sophisticated layout design.

Cascode topology comprises of two transistors in common-source and common-gate configuration, respectively. The unique structure benefits to decreased Miller feedback capacitance, preferable power gain and output impedance. Further, coplanar waveguide (CPW) technique is compatible with Cascode topology, and importantly it is simplified without backside processing. Therefore, Cascode topology and CPW technique are widely used in various millimeter-wave applications^[6-7].

In this paper, a single-stage W-band LNA MMIC in Cascode topology is reported with high linear gain of 15.2 dB at 95 GHz and optimal noise figure of 4.3 dB at 87.5 GHz at room temperature. Specifically, this LNA MMIC exhibits the highest gain-per-stage and competitive gain-area ratio among reported W-band LNA MMICs. Additionally, the amplifier also demonstrates a high saturated power of 8.05 dBm at 88 GHz. The successful fabrication of LNA MMIC is of great significance on building a W-band signal receiver-front-end system.

1 InP HEMT technology

The single-stage W-band LNA MMIC was developed in our own InP-based HEMT technology, which was outlined in previous articles^[8-10]. HEMTs with gate-width of $2 \times 50 \mu\text{m}$ and gate-length of $0.15 \mu\text{m}$ were employed for the LNA MMIC design. According to preliminary noise parameters and S-parameters measurements, the best trading-off between noise property and gain performance was obtained at $V_{GS} = 0.1 \text{ V}$, $V_{DS} = 1.5 \text{ V}$ and $I_{DS} = 106 \text{ mA/mm}$. Meanwhile the current gain cutoff frequency (f_T) and maximum oscillation frequency (f_{max}) are 126 GHz and 320 GHz, respectively. Additionally, MMIC technology includes $0.3 \text{ fF}/\mu\text{m}^2$ metal insulator metal (MIM) capacitors, $50 \Omega/\text{sq}$ thin film resistors (TFRs). CPW transmission lines. Besides, air-bridges were utilized at CPW discontinuous interface to inhibit non-ideal slot mode excitation effect. Specially, the cross-sectional profile of MMIC manufacturing technology is plotted in Fig. 1.

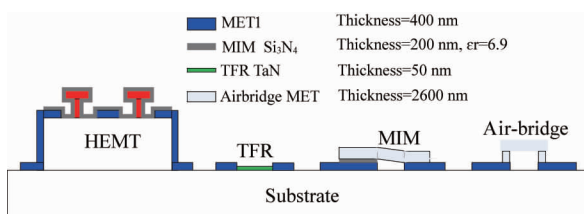


Fig. 1 Cross-sectional profile of InP-based HEMT MMIC technology

图1 InP基HEMT MMIC工艺剖面图

2 LNA design

2.1 Cascode structure

The maxgain for common source and Cascode structure is depicted in Fig. 2, and it is 11.235 dB at 96 GHz for common source structure, which improves to

19.129 dB for Cascode structure. The improved feedback capacitance and output conductance benefit to gain performance of Cascode architecture, however, the stability becomes a thorny problem worthy of attention. In order to stabilize amplifier, approximate high-impedance transmission line can be introduced to connect common-source transistor and common-gate transistor, which provides significant inductive peaking to compensate for the capacitive impedance and gain rolling off characteristics. Additionally, the RF grounding capacitance for second gate should be determined with stability in consideration.

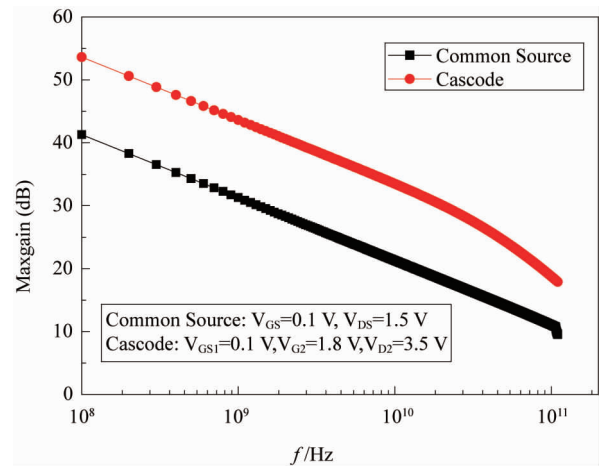


Fig. 2 The maxgain for common source and cascode structure

图2 共源和共源共栅结构的增益性能

2.2 LNA design

The small-signal noise model utilized in LNA design is extrapolated from S-parameters up to 40 GHz and noise parameters to 18 GHz. Two InP-based HEMTs are designed in common-source and common-gate structures. The schematic diagram of W-band cascode LNA is illustrated in Fig. 3, which comprises of Cascode core, bias lines, input matching network, and output matching network.

The LNA MMIC is designed through co-simulating of schematic and electromagnetic field in Advanced Design System (ADS) software from Agilent Technologies. Firstly, Cascode core is designed by trading-off gain and stability in operating frequencies through optimizing high-impedance transmission line and RF grounding capacitance. Secondly, the optimum source impedance (Z_{opt}) of $15 + j9.6$ is determined for minimum noise figure, while the load impedance (Z_{Load}) of $9.6 + j56.3$ for maximum gain. Thirdly, the input and output matching network topologies are both proposed to be open stub network topology in Smith chart. Fourthly, the bias lines are designed with quarter-wave short stubs at a center frequency of 94 GHz, and the bypass MIM capacitors short-out millimeter-wave signals. In addition, TFR and capacitors are shunted at the end of bias networks to improve low frequency stability. Fifthly, the capacitors, TFRs, and CPWs are optimized by compromising among gain, noise and stability. Stability is a necessary precondition for all integrated circuits in high frequencies, which relates directly to the circuits' success or failure.

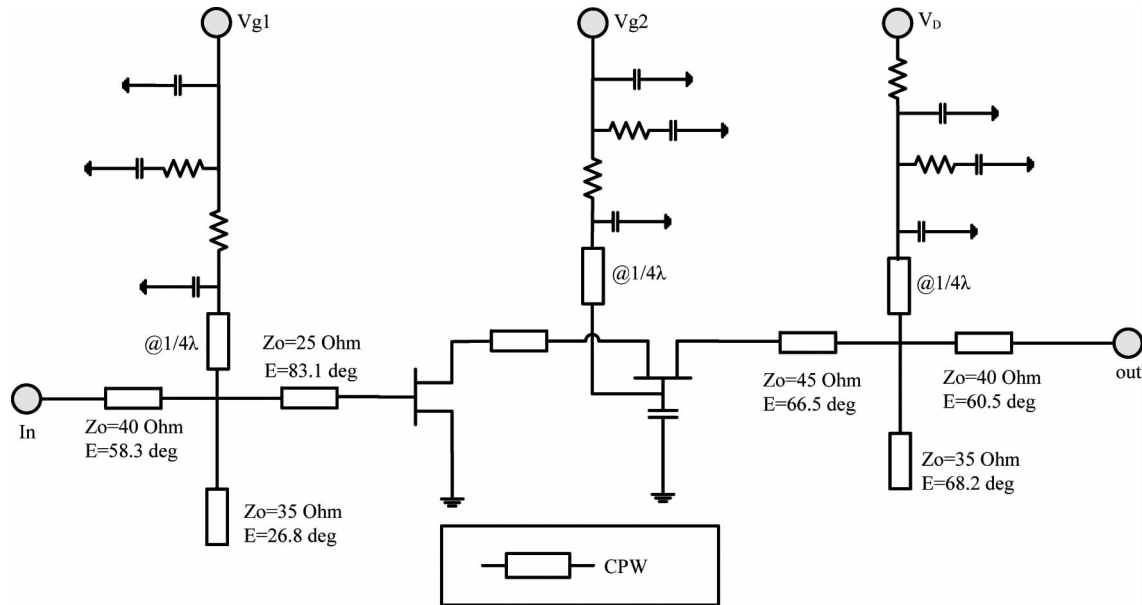


Fig. 3 Circuit topology for the cascode LNA

图3 共源共栅 LNA 电路拓扑结构

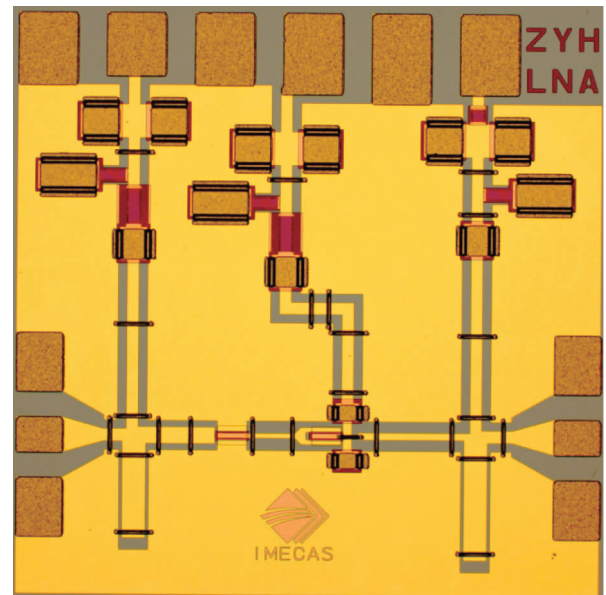
Thus, it is even worthy to sacrifice some gain to achieve further circuit stability in a sense. Therefore, the Rollett stability factor K is given a higher weight in LNA optimization procedure, and finally it far exceeds 1 over all frequencies from DC to 100 GHz.

In the layout design process, ground-to-ground spacing of CPW lines is fixed as $50 \mu\text{m}$. The cascode core, output matching network, input matching network and bias networks are designed separately by using electromagnetic (EM) simulator module of Momentum in ADS. Finally, the entire designed circuit is EM-simulated together. Figure 4 shows photograph of the W-band LNA MMIC. The cascode topology and coplanar layout lead to a compact chip with size of $900 \mu\text{m} \times 975 \mu\text{m}$.

3 Measurement and discussion

On-wafer S-parameters of the LNA MMIC were characterized with HP8510C vector network analyzer and on W-band semi-automatic probe station of SUSS Micro-Tec. To measure noise figure (NF), W-band output signal was down-converted and measured by N8975A NFA series noise figure analyzer in frequencies from 10 MHz to 26.5 GHz. The output power performances were measured by adopting a W-band power meter and a multi-frequency source with a signal generator (E8257D, 250 ~ 40 GHz). The W-band LNA MMIC was biased for the best trading-off between low noise figure and high gain, under $V_{D2} = 3.5 \text{ V}$, $V_{GS1} = 0.1 \text{ V}$ and $V_{G2} = 1.8 \text{ V}$, while the entire drain current was 10.6 mA.

On-wafer S-parameters measured at room temperature are depicted in Fig. 5. The maximum linear gain of approximately 13 dB is obtained at 92.5 GHz. In 80-96 GHz frequency range, the small-signal gain is far larger than 10 dB. The measured input return loss (S_{11}) and output return loss (S_{22}) are better than -14 dB and -7 dB in operating frequencies, respectively, which ensuring

Fig. 4 Microphotograph of the cascode LNA with over-all chip-size of $900 \mu\text{m} \times 975 \mu\text{m}$ 图4 共源共栅 LNA 显微镜照片(芯片面积为 $900 \mu\text{m} \times 975 \mu\text{m}$)

superior standing wave ratio. Admittedly the maximum gain and corresponding operating frequency slightly shift toward negative direction from the simulated with the maximum gain of 16.6 dB at 96 GHz, but extraordinary identical tendency between measurement and simulation could be detected. In particular, the input signal power is about -12 dBm from vector network analyzer. In this case, LNA MMIC might be gain-compressed, which is accurately verified by the noise performance measurement with small enough input signal of W-band noise source.

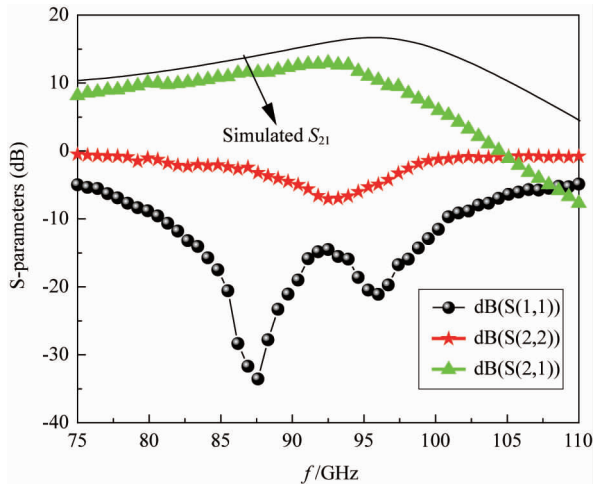


Fig. 5 Measured S-parameters of the Cascode LNA MMIC
图5 共源共栅 LNA MMIC 芯片的 S 参数

Figure 6 shows the associated gain and noise figure of the single-stage LNA MMIC measured in W-band at room temperature. The LNA exhibits excellent linear gain of better than 10 dB from 84 GHz to 100 GHz with the peak value of 15.2 dB at 95 GHz. The input signal power from noise source is so extremely small as to ensure associated gain of the LNA MMIC be real small-signal gain without any doubt. Furthermore, the optimal noise figure of 4.3 dB with relatively high associated gain of 12 dB is acquired at 87.5 GHz. Inaccurate technology process and inadequate simulation of uncommon coupling factor might result in gain slightly decreasing and the center frequency shifting. Especially, the output impedance of Cascode pair is situated around the edge in Smith chart, so slightly inaccurate process would result in the output mismatching, and finally seriously impacts the S-parameters of amplifier.

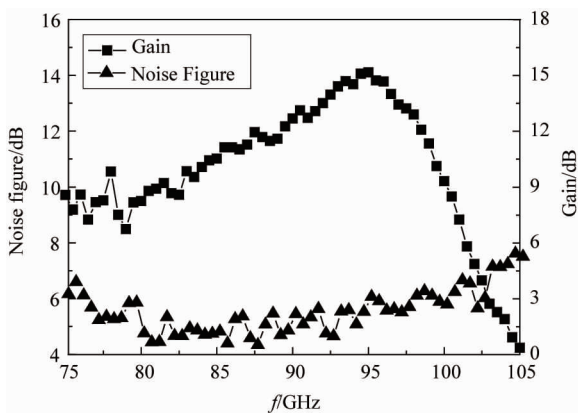


Fig. 6 Associated gain and noise figure of the cascode LNA MMIC

图6 共源共栅 LNA MMIC 增益和噪声特性

Table 1 shows a detail comparison with reported W-band LNA MMICs in various technologies. This single-stage LNA MMIC exhibits the highest gain-per-stage and competitive gain-area ratio among reported W-band LNA

MMICs. Primarily, our InP-based HEMT possesses a relatively high f_{max} , which indicates high gain performance. Additionally, the improved feedback capacitance and output conductance benefit to gain performance of Cascode architecture. However, noise performance is slightly inferior to other publishes. Probably, 200 nm Si_xN passivation layer deposited at high temperature results in much higher pinch-off voltage (V_{th}), then large gate leakage current necessitated comparatively poor noise performance. Simultaneously, apparent degraded parasitic resistance for the passivated device becomes another noise source.

Table 1 Comparison of the W-band HEMT LNAs

表1 W 波段 HEMT LNAs 的比较

NF(dB)	Gain (dB)	Stage	Chip-size(mm ²)	Device(f_{max})	Reference
2.5	5.6	1	1.1 × 1.1	ABCS(190 GHz)	[11]
4.7	14.8	1	1.8 × 1.48	MHEMT(305 GHz)	[12]
2.8	18.5	3	1 × 1.75	MHEMT(670 GHz)	[13]
3.5	18	3	0.55 × 0.75	InP HEMT(283 GHz)	[14]
~	21.2	5	3.2 × 1.7	InP HEMT(270 GHz)	[15]
4.3	15.2	1	0.900 × 0.975	InP HEMT(320 GHz)	This work

Apart from gain and noise characteristics, the output power of amplifier should be large enough to drive subsequent circuit in a system. In power characteristics measurement, the loss of connection components, including waveguide and probe was calibrated by the calibrator. The input power of the LNA MMIC was configured between -3 ~ 2 dBm from 75 to 100 GHz by adjusting the attenuator before amplifier. The saturated output power of the W-band Cascode LNA MMIC is plotted in Fig. 7. The amplifier has demonstrated a peak output power of 8.05 dBm with -0.06 dBm input power at 88 GHz.

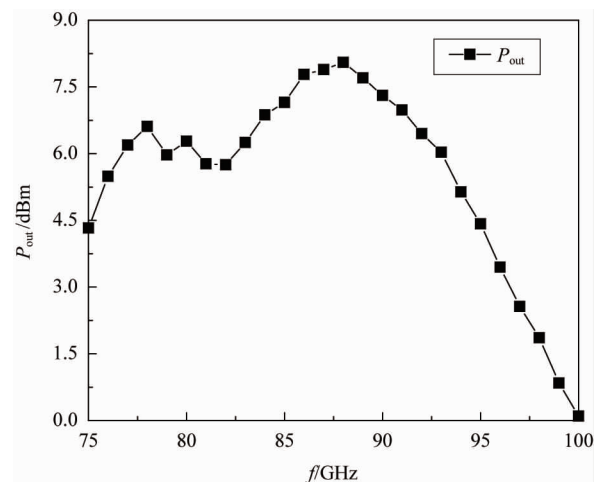


Fig. 7 The measured saturated output power of the single-stage cascode LNA MMIC

图7 单级共源共栅 LNA MMIC 芯片的饱和输出功率

4 Conclusions

A single-stage W-band cascode LNA MMIC has been designed and developed using our own InP-based HEMT technology. The LNA MMIC exhibits significantly

high linear gain of 15.2 dB at 95 GHz with peak saturated output power of 8.05 dBm at 88 GHz, and achieves the optimum noise figure of 4.3 dB with relatively high associated gain of 12 dB at 87.5 GHz. Specifically, the LNA MMIC possesses the highest gain-per-stage and competitive gain-area ratio among reported W-band LNA MMICs. In order to further improve noise performance, shorter gate-width device can be used to decrease drain-source channel current. However, these results undoubtedly illustrate that the InP-based HEMT technology is exceedingly appropriate for various low noise and high gain millimeter-wave applications.

Acknowledgement

The authors would like to express heartfelt thanks to Ouyang Sihua and Li Yankui for tuning the measurement equipments, meanwhile, the authors are very grateful for all the members in Compound Semiconductor Device Department, Institute of Microelectronics, Chinese Academy of Sciences.

References

- [1] Floyd B A, Reynolds S K, Preiffer U R, *et al.* SiGe bipolar transceiver circuits operating at 60 GHz[J]. *IEEE Journal Solid-State Circuits*, 2005, **40**(1): 156–167.
- [2] Li W, Kraemer R, Borngraerber J. An improved highly-linear low-power down-conversion micromixer for 77 GHz automotive radar in SiGe technology[C]. *IEEE MTT-S Int Microw Symp Dig*, San Francisco, CA, 2006: 1834–1837.
- [3] Vizard D R, Doyle R. Advances in millimeter wave imaging and radar systems for civil applications[C]. *IEEE MTT-S Int Microw Symp Dig*, San Francisco, CA, 2006: 94–97.
- [4] Sato M, Hirose T, Ohki T, *et al.* 94-GHz Band high-gain and low-noise amplifier using InP-HEMTs for passive millimeter wave imager [C]. *IEEE MTT-S Int Microw Symp Dig*, Honolulu, HI, 2007: 1775–1778.
- [5] Mei X B, Lin C H, Lee L J, *et al.* A W-Band InGaAs/InAlAs/InP HEMT low-noise amplifier MMIC with 2.5 dB noise figure and 19.4 dB gain at 94 GHz [C]. 20th International Conference on Indium Phosphide and Related Materials (IPRM), Versailles, 2008: 1–3.
- [6] Zhong Y H, Zhang Y M, Zhang Y M, *et al.* A W-band two-stage cascode amplifier with gain of 25.7 dB[J]. *Journal of Semiconductors*, 2013, **34**(12): 125003–1.
- [7] Deal W R, Leong K, Mei X B, *et al.* Scaling of InP HEMT cascode integrated circuits to THz frequencies[C]. *IEEE Compound Semiconductor Integrated Circuit Symposium (CSICS)*, 2010. Monterey, CA, 2010: 1–4.
- [8] ZHONG Ying-Hui, WANG Xian-Tai, SU Yong-bo, *et al.* High performance InP-based $\text{In}_{0.52}\text{Al}_{0.48}\text{As}/\text{In}_{0.53}\text{Ga}_{0.47}\text{As}$ HEMTs with extrinsic transconductance of 1 052 mS/mm[J]. *Journal of Infrared and Millimeter Waves* (钟英辉, 王显泰, 苏永波, 等. 有效跨导为 1 052 mS/mm 的高性能 InP 基 $\text{In}_{0.52}\text{Al}_{0.48}\text{As}/\text{In}_{0.53}\text{Ga}_{0.47}\text{As}$ HEMTs, 红外与毫米波学报), 2013, **32**(3): 193–197.
- [9] Zhong Y H, Zhang Y M, Zhang Y M, *et al.* 0.15 μm T-gate $\text{In}_{0.52}\text{Al}_{0.48}\text{As}/\text{In}_{0.53}\text{Ga}_{0.47}\text{As}$ InP-based HEMT with f_{max} of 390 GHz[J]. *Chinese Physics B*, 2013, **22**(12): 128503–5.
- [10] Zhong Y H, Yang J, Li X J, *et al.* Impact of the silicon-nitride passivation film thickness on the characteristics of InAlAs/InGaAs InP-based HEMTs[J]. *Journal of the Korean Physical Society*, 2015, **66**(6): 1020–1024.
- [11] Riemer P J, Buhrow B R, Hacker J B, *et al.* Low power W-band CPWG InAs/AlSb HEMT low-noise amplifier[J]. *IEEE Microwave and Wireless Components Letters*, 2006, **16**(1): 40–42.
- [12] Pyu K-K, Kim S-C, An D, *et al.* High-performance CPW MMIC LNA using GaAs-based metamorphic HEMTs for 94-GHz applications[J]. *Journal of The Korean Physical Society*, 2010, **56**(5): 1509–1513.
- [13] Thome F, Massler H, Wagner S, *et al.* Comparison of two W-band low-noise amplifier MMICs with ultra low power consumption based on 50 nm InGaAs mHEMT technology [C]. *IEEE MTT-S International Microwave Symposium Digest*, Seattle, WA, 2013: 1–4.
- [14] Sato M, Takahashi T, Hirose T. 68-110 GHz band low-noise amplifier using current reuse topology[J]. *IEEE Transaction on Microwave Theory and Techniques*, 2010, **58**(7): 1910–1916.
- [15] Liang L, Alt A R, Benedickter H, *et al.* Low power consumption millimeter-wave amplifiers using InP HEMT technology[C]. *IEEE MTT-S International Microwave Workshop Series on Millimeter Wave Integration Technologies*. Sitges, 2011: 9–12.